Biophys Rev
DOI 10.1007/s12551-013-0101-7

REVIEW

Simulation and modeling of crowding effects on the thermodynamic and kinetic properties of proteins with atomic details

Huan-Xiang Zhou · Sanbo Qin

Received: 19 November 2012 / Accepted: 16 January 2013

Abstract Recent experimental studies of protein folding and binding under crowded solutions suggest that crowding agents exert subtle influences on the thermodynamic and kinetic properties of the proteins. While some of the crowding effects can be understood qualitatively from simple models of the proteins, quantitative rationalization of these effects requires an atomistic representation of the protein molecules in modeling their interactions with crowders. A computational approach, known as postprocessing, has opened the door for atomistic modeling of crowding effects. This review summarizes the applications of the postprocessing approach for studying crowding effects on the thermodynamics and kinetics of protein folding, conformational transition, and binding. The integration of atomistic modeling with experiments in crowded solutions promises new insight into biochemical processes in cellular environments.

Keywords Macromolecular crowding · Protein folding · Protein binding · Simulation · Modeling · Postprocessing

Introduction

The idea that the crowded conditions of cellular environments can significantly affect the biophysical properties of proteins and nucleic acids, promoted by Minton and others (Zimmerman and Minton 1993; Kornberg 2000; Ellis 2001; Zhou et al. 2008), is now bearing many fruits. The biophysical community is largely convinced of the affirmative answer to the question of whether macromolecular crowding makes important contributions to cellular functions, and is now working on the characterization and quantification of these contributions, as well as on developing tools and techniques for modeling these contributions experimentally, theoretically, and through simulation (Elcock 2010). This review focuses on recent progress in our understanding of macromolecular crowding achieved through molecular simulations, with a particular focus on the effects of crowding, calculated through an approach known as postprocessing (Qin and Zhou 2009; Qin et al. 2010), on the thermodynamics and kinetics of protein folding, conformational transition, and binding.

Many experimental studies have been directed at measuring the degree to which crowding agents affect the folding, conformational transition and binding equilibria (Qu and Bolen 2002; Spencer et al. 2005; Roberts and Jackson 2007; Batra et al. 2009a, b; Phillip et al. 2009; Dhar et al. 2010; Miklos et al. 2011; Denos et al. 2012), often spurred by Minton's predictions of significant crowder-induced stabilization of the compact states over the more open states (Minton 1981, 1998, 2000, 2005). The predictions are largely based on the scaled particle theory (Lebowitz and Rowlinson 1964) for the free energy of transferring a test protein into crowders, all of which are modeled as convex hard particles. The experimental results have often validated the qualitative aspect of Minton's predictions, but the observed magnitudes of crowding effects are usually smaller than anticipated. Moreover, the subtle and complicated influences of crowding agents revealed by some experiments, such as a dependence on the chemical nature of the crowders (Batra et al. 2009b; Miklos et al. 2011; Denos et al. 2012), seem to be beyond the scope of simple theoretical models. Recent experiments on the kinetics of protein folding and binding under crowded conditions (Kuttner et al. 2005; Schlarb-Ridley et al. 2005; Ai et al. 2006; Yuan et al.

Special Issue: Protein-Protein and Protein-Ligand Interactions in Dilute and Crowded Solution Conditions. In Honor of Allen Minton's 70th Birthday

H.-X. Zhou (✉) · S. Qin
Department of Physics and Institute of Molecular Biophysics, Florida State University, Tallahassee, FL 32306, USA
e-mail: hzhou4@fsu.edu

Published online: 16 February 2013

2008; Phillip et al. 2009, 2012a; Denos et al. 2012) pose additional challenges, since the effects of crowders on the thermodynamics and dynamics of test proteins can potentially oppose each other, leading to a net effect on the kinetics that is even more moderated than that on the equilibria (Zhou 2004; Qin et al. 2012).

Molecular simulations have further enriched our understanding of protein folding, conformational transition, and binding under crowding conditions. Earlier studies took the direct simulation approach (horizontal paths in Fig. 1a), i.e., as in an in vitro experiment, the test protein(s) in a biochemical process of interest and the crowders are simulated together (Fig. 1b). Because the simulation had to include a large number of crowder molecules and was designed to model rare transitions between stable states along the biochemical process, the test protein(s) by necessity was (were) represented at the coarse-grained level (e.g., one bead per residue) (Cheung et al. 2005; Minh et al. 2006; Kim et al. 2010; Mittal and Best 2010). The alternative, postprocessing approach (vertical paths in Fig. 1a) (Qin and Zhou 2009; McGuffee and Elcock 2010; Qin et al. 2010) circumvents the modeling of rare transitions between stable states and has allowed the test proteins to be represented at the all-atom level (Fig. 1c). Such atomistic modeling enables more quantitative interrogation by and closer integration with experimental studies of crowding effects, hopefully leading to new insight into biochemical processes in cellular environments.

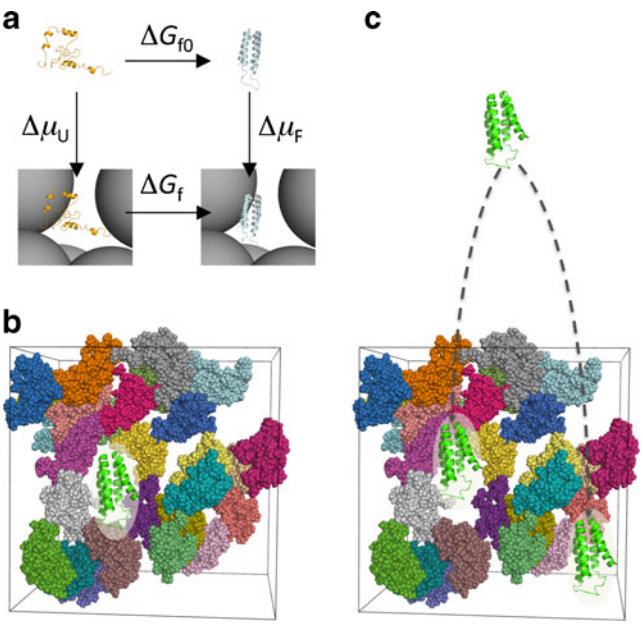

Fig. 1 Two different approaches for modeling biochemical reactions under crowding. **a** The direct simulation approach follows the horizontal paths, whereas the postprocessing approach follows the vertical paths, illustrated on the folding process of cytochrome b_{562}. The same free energy difference ($\Delta\Delta G$), here representing the effect of crowding on the folding free energy, is obtained by following either the horizontal paths ($\Delta\Delta G=\Delta G_f - \Delta G_{f0}$) or the vertical paths ($\Delta\Delta G=\Delta\mu_F - \Delta\mu_U$) (Zhou et al. 2008). **b** In the direct simulation approach, the folding transition is followed in the presence of crowders. **c** In the postprocessing approach, only the folded state and the unfolded state are simulated, not their inter-conversion, and the simulations are done in the absence of crowders (Qin and Zhou 2009). Snapshots of the folded (unfolded) protein are then fictitiously inserted into the crowders to calculate $\Delta\mu_F$ ($\Delta\mu_U$)

Modeling crowding by direct simulations

Using direct simulations, Cheung et al. (2005) studied the folding stability and kinetics of the 34-residue all-β WW domain in the presence of purely repulsive spherical crowders. The WW domain was coarse-grained to two beads per residue (representing the Cα atom and the center of mass of the side chain), with a Go-like potential (Ueda et al. 1978) in which only native interactions were retained. At a crowder volume fraction (ϕ) of 0.25, the melting temperature was increased by as much as 24 °C. In contrast to the crowding effect on folding stability, the folding rate constant (k_f) exhibited a non-monotonic dependence in ϕ, reaching a maximum of a threefold increase at ϕ=0.1 (relative to the crowder-free situation) and then slowing down to a 1.8-fold increase. Cheung et al. (2005) attributed the latter slowing down to restricted conformational fluctuations needed for the folding transition.

A similar model was adopted by Mittal and Best (2010) to study the effect of crowding on the folding free energy surfaces of three small proteins. The potentials of mean force along the fraction of native contacts were obtained by umbrella sampling. For each protein, crowding increased the free energy of the unfolded state well relative to that of the folded state well. Also using direct simulations, Minh et al. (2006) studied the effect of crowding on the flap opening equilibrium of the HIV-1 protease dimer. The opening motion is essential for substrate and inhibitor binding. These researchers found that repulsive crowders decreased the flap-open population.

Feig and Sugita (2012) recently carried out all-atom explicit solvent molecular dynamics simulations of chymotrypsin 2 (CI2) in the presence of either lysozyme or bovine serum albumin as crowders. These simulations were motivated by the experiments of Miklos et al. (2011), who used nuclear magnetic resonance-detected amide proton exchange to probe residue-level local stability, i.e., the stability of individual residues to withstand opening up for hydrogen/deuterium exchange (Englander and Kallenbach 1983). Opening of the residues with the highest local stability involves global unfolding; hence, the highest local stability corresponds to the folding stability. The experiments showed that the protein crowders decreased the local stability of many of the monitored CI2 residues and the folding stability, in contrast to an increase in folding stability by

polymer crowders on CI2 and on a number of other proteins. Miklos et al. (2011) attributed the decreased local and folding stability to attractive interactions between the test protein and the crowder protein molecules. The work of Feig and Sugita (2012) corroborated this attribution, in that the residues showing decreased local stability largely overlap with residues showing increased conformational fluctuations in the simulations in the presence of the protein crowders. It should be noted that the simulations of the Feig and Sugita (2012) probe nanosecond fluctuations in the folded state, whereas the experiments of Miklos et al. (2011) present measurements on the equilibria between the folded state and the locally or globally unfolded state. A re-analysis of these measurements has now suggested experimental temperature as a contributing factor for the observed differences, and that all of the data can be explained by a unified mechanism of action for protein and polymer crowders (Zhou 2013).

Postprocessing approach: strategy and implementation

Instead of following the horizontal paths of Fig. 1a to obtain $\Delta\Delta G$, the effect of crowding on the free energy change of the test protein(s) in a biochemical process (folding, conformational change, or binding), in the postprocessing approach we follow the vertical paths. That is, we calculate the free energy for transferring, from a dilute solution to a crowded solution, the protein(s) either in the reactant state or the product state (Qin and Zhou 2009; Qin et al. 2010). By closing a thermodynamic cycle, the difference between the two transfer free energies is the same as the $\Delta\Delta G$ between the two horizontal paths, but we avoid simulating rare transitions along the horizontal paths.

To implement the postprocessing approach, we carry out separate simulations for the test proteins(s) in the reactant state and in the product state, without any crowders. The latter condition allows the test proteins to be represented at the all-atom level and the simulations to be done in an explicit solvent. A separate simulation of the crowder molecules is also carried out to generate a configurational ensemble for the crowded solution and can be used for the transfer of many test proteins.

To calculate the transfer free energy ($\Delta\mu$) of the test protein(s) in a given state, we take snapshots from the simulation in that state and fictitiously insert them into the crowded solution (Fig. 1c). If the effective interaction energy between a test protein and the crowders is $U(\mathbf{X}, \mathbf{R}, \mathbf{\Omega})$, where $\mathbf{X}$, $\mathbf{R}$, and $\mathbf{\Omega}$ represent the conformation, position, and orientation, respectively, of the test protein, then $\Delta\mu$ is given by

$$\exp(-\Delta\mu/k_{\mathrm{B}}T) = <\exp[-U(\mathbf{X},\mathbf{R},\Omega)/k_{\mathrm{B}}T]>_0 \qquad (1)$$

where k_{B} is Boltzmann's constant, T is the absolute temperature, $<\cdots>_0$ means averaging over the conformation, position, and orientation of the test protein and over the configurations of the crowders, and the subscript "0" emphasizes the fact that the protein conformations are those sampled in the absence of crowders. Postprocessing is simply a form of Widom's insertion method (Widom 1963). For the purely repulsive interaction between crowders and test proteins, $U(\mathbf{X}, \mathbf{R}, \mathbf{\Omega})$ is either 0, when the test protein does not clash with crowders, or infinite, when a clash occurs. Correspondingly, $\exp[-U(\mathbf{X}, \mathbf{R}, \mathbf{\Omega})/k_{\mathrm{B}}T]$ is either 1 or 0, and the average on the right-hand side of Eq. (1) is the clash-free or allowed fraction (f) of attempts to insert the test protein into the crowded solution.

The allowed fraction of insertion can be simply calculated by repeatedly inserting the test protein into the crowded solution and testing for clash, but we have designed an algorithm to speed up the calculation for spherical crowders (Qin and Zhou 2009). Briefly, we take one crowder particle and identify all of the grid points at which the placement of the test protein (in a given conformation and orientation) results in clash. We then copy all the "clashing" grid points to each crowder particle in the crowded solution (in a given crowder configuration). The allowed fraction of insertion is finally given by the fraction of grid points that are not part of the clashing grid points of any crowder particle. The calculation needs to be repeated for other test protein conformations and orientations and other crowder configurations to obtain the appropriate average.

Because the calculation needs to be repeated many times, we further developed an alternative, faster way of calculating the transfer free energy (Qin and Zhou 2010). We were guided by the observation that the transfer free energies calculated by our insertion algorithm can be fitted to the scaled particle theory with the radius, surface area, volume of the test protein as free parameters; the fitted values of these parameters are more or less those expected from the structure of the protein (Batra et al. 2009a; Qin and Zhou 2009). Mittal and Best (2010) confirmed this observation in their subsequent study. Essentially, our calculation for the transfer free energy can be viewed as a generalization of the fundamental measure theory (Rosenfeld 1989; Oversteegen and Roth 2005), which itself is a generalization of the scaled particle theory. Our generalized fundamental measure theory (GFMT) predicts the transfer free energy as

$$\Delta\mu = \prod_{\mathrm{c}} v_{\mathrm{p}} + \gamma_{\mathrm{c}} s_{\mathrm{p}} + \kappa_{\mathrm{c}} l_{\mathrm{p}} - k_{\mathrm{B}}T\ 1\mathrm{n}(1-\phi) \qquad (2)$$

where v_{p}, s_{p}, and l_{p} are the volume, surface area, and linear size, respectively, of the test protein, and Π_{c}, γ_{c}, and κ_{c} are the osmotic pressure, surface tension, and bending rigidity, respectively, of the crowded solution. The latter crowder-only quantities are determined by the volume, surface area, and radius of the crowders. The geometric quantities v_{p}, s_{p}, and l_{p} of the test protein are

essentially defined by its crowder-excluded surface (represented at the all-atom level). Note that the crowder-excluded surface depends on the crowder radius and is not convex. Figure 2 illustrates the good agreement between the GFMT transfer free energies and those calculated by the insertion algorithm.

Validation against direct simulations

In essence the postprocessing approach yields the transfer free energy by using the protein conformations sampled in the absence of crowders and reweighting them according to the would-be protein-crowder interaction energy. Of course, the important conformational region will necessarily shift due to the presence of crowders. The postprocessing calculation is exact if the conformational space of the protein is exhaustively sampled so as to cover the important conformational region in the presence of crowders. In practice, however, can conformations be adequately sampled to ensure accurate calculation by the postprocessing approach? An important test case is whether the conformations sampled in the absence of crowders through the direct simulation approach can be used to predict crowding effects.

We recently addressed such a test case (Qin et al. 2010). Using the simulation code of Minh et al. (2006) we extended their study of the effect of crowding on the flap opening equilibrium of the HIV-1 protease dimer. The values of the flap-open probability (p_o) calculated using the direct simulation approach at 8 volume fractions of 30-Å crowders are shown in Fig. 3 as *circles*. p_o shows a small but distinct decrease with increasing ϕ. Using only the conformations sampled in the absence of crowders and applying postprocessing, we reproduced the direct simulation results very well (*curve* in Fig. 3). While the direct simulation results have significant statistical errors (as estimated by the variation among 6 repeat simulations), the statistical errors of the postprocessing approach on the crowding effect are negligible. The significant reduction in statistical errors comes about because averaging over protein position and orientation and over crowder configuration is effectively exhaustive in the postprocessing approach (Qin and Zhou 2009).

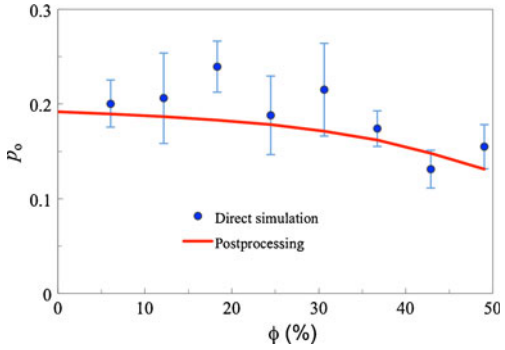

Fig. 3 Postprocessing predictions (*curve*) and direct simulation results (*circles*) for the HIV-1 protease dimer flap-open probability under crowding, taken from Qin et al. (2010). *Error bars* in the direct simulation results represent variations among 6 repeat simulations. The postprocessing results are predicted according to $p_o/p_c = \exp[-(\Delta\mu_o - \Delta\mu_c)/k_BT]p_{o0}/p_{c0}$, where p_o and p_c are the flap-open and flap-close probabilities under crowding, p_{o0} and p_{c0} are the counterparts in the absence of crowding, and $\Delta\mu_o$ and $\Delta\mu_c$ are the transfer free energies of the open and closed conformational ensembles

In the postprocessing approach, the same conformations, sampled in the absence of crowders, are used for different crowding conditions, such as the different volume fractions of the 30-Å crowders (Fig. 3) or for crowders with other sizes. For 100-Å crowders, the decrease in p_o with increasing ϕ becomes negligible. The latter prediction explains the experimental observation that 6 % Ficoll400 (with a Stokes

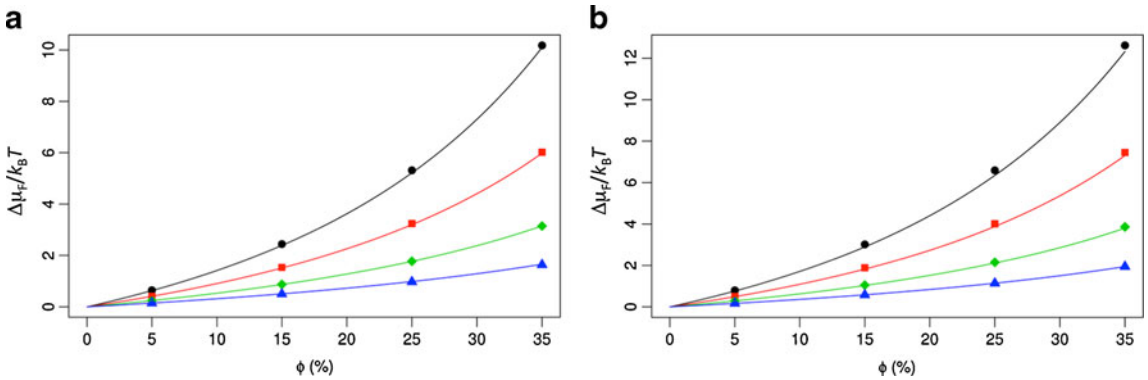

Fig. 2 Comparison of the generalized fundamental measure theory (GFMT) results and those calculated by the insertion algorithm (Qin and Zhou 2009) for the transfer free energies of cytochrome b_{562} in the folded state (**a**) and unfolded state (**b**). The results by the insertion algorithm are shown as *circles*, *squares*, *diamonds*, and *triangles* for crowders with radii of 15, 20, 30, and 50 Å, respectively; the corresponding GFMT results are shown as *curves*. These results were calculated in Qin and Zhou (2010), but there only the difference between $\Delta\mu_F$ and $\Delta\mu_U$ was shown. The GFMT calculations yielded values of 21.1, 21.4, and 21.8 Å for the linear size (l_p) of cytochrome b_{562} in the folded state when the crowder radii were 15, 30, and 50 Å, respectively; the corresponding values of l_p were 24.5, 25.4, and 25.9 Å in the unfolded state. Note that these values corresponding to different crowder radii were obtained from the same set of protein conformations (either in the folded or unfolded state) generated without crowders

radius of approx. 100 Å) did not result in a discernible change in the distribution of the inter-flap distance (Galiano et al. 2009). Using the postprocessing approach, we have also been able to reproduce Mittal and Best's (2010) direct simulation results for the folding free energy surfaces of three small proteins under crowding (Qin et al. 2013).

From theymodynamics to kinetics

In addition to equilibrium properties, the postprocessing approach can be applied to model crowding effects on kinetic properties. In general, the rate constant of a biochemical reaction is determined by the energetics and dynamics of the biomolecule(s) involved (Zhou 2010). The rate constant under crowding can be modeled by accounting for the effects of crowding on these energetic and dynamic properties (Zhou 2004; Qin et al. 2012).

The rate constant for a unimolecular reaction, such as a folding or unfolding process or a conformational transition, can generally be expressed as (Zhou 2010)

$$k = A \exp\left(-\Delta G^{\ddagger}/k_{\mathrm{B}}T\right) \tag{3}$$

where $\Delta G^{\ddagger}$ is the activation energy (i.e., difference in free energy between the transition state and the reactant state), and A is a prefactor dictated by the dynamics, which can be described as diffusive for most biochemical reactions, along the reaction coordinate. Both internal dynamics and the solvent microviscosity can contribute to the effective diffusion constant along the reaction coordinate (Ansari et al. 1992). In principle, crowding can affect both $\Delta G^{\ddagger}$ and the prefactor A. The effect of crowding on $\Delta G^{\ddagger}$ can be calculated by the postprocessing approach, just as described above for the free energy difference between two stable states, provided that we can sample the transition state (in the absence of crowders) in addition to the reactant state.

The effect of crowding on A depends on the extent to which the reaction coordinate is exposed to crowders. In one extreme, the motion leading to the transition state involves only residues that are shielded from crowders, then A should be relatively independent of crowding (Yuan et al. 2008). As another example, the folding rate constant of a small protein calculated by Mittal and Best (2010) through simulations was consistent with that predicted when only the effect of crowding on the free energy surface was taken into consideration. In the other extreme, the rate-limiting step involves large-scale relative motion between domains or large fragments of the protein; in this case, crowders will affect A by changing the microviscosity. (Note that, for macromolecular crowders, the microviscosity is usually much less than the bulk viscosity.) If the relative translational diffusion constant of the domains changes from D_0 to D under crowding, then we expect the prefactor to change in proportion:

$$\frac{A}{A_0} = \frac{D}{D_0} \tag{4}$$

In general, we expect the effect of crowding on A to fall between the above two extremes.

Protein–protein binding can be reaction-limited, diffusion-limited, or between these two regimes. In the reaction-limited regime, the rate-limiting step is the crossing of an energy barrier, much like in a unimolecular reaction. This may involve conformational rearrangement of one of both proteins during the binding process. The effect of crowding on the binding rate constant in the reaction-limited regime can be modeled very similarly to what is described above for unimolecular reactions.

For binding in the diffusion-controlled regime, we have developed a computational method known as the transient-complex theory for predicting the rate constant (Alsallaq and Zhou 2008; Qin et al. 2011). The transient complex refers to an intermediate in which the two proteins have near-native separation and relative orientation but have yet to form most of the short-range native interactions. The association rate constant is predicted as

$$k_{\mathrm{a0}} = k_{\mathrm{a0}}^{0} \exp\left(-\Delta G_{\mathrm{el}}^{\star}/k_{\mathrm{B}}T\right) \tag{5}$$

where k_{a0}^{0} is the basal rate constant, i.e., the rate constant for reaching the transient complex by unbiased diffusion, and the Boltzmann factor (with $\Delta G_{\mathrm{el}}^{\star}$ denoting the electrostatic interaction energy in the transient complex) accounts for the biasing contribution of long-range electrostatic interactions in the diffusional approach to the transient complex. We have now extended the transient-complex theory to account for the effects of crowding (Qin et al. 2012). Crowding modifies the basal rate constant (from k_{a0}^{0} to k_{a}^{0}) by changing the microviscosity and induces an effective interaction energy ($\Delta\Delta G_{\mathrm{c}}$) between the proteins. Therefore

$$k_{\mathrm{a}} = k_{\mathrm{a}}^{0} \exp\left(-\Delta G_{\mathrm{el}}^{\star}/k_{\mathrm{B}}T\right) \exp\left(-\Delta\Delta G_{\mathrm{c}}^{\star}/k_{\mathrm{B}}T\right) \tag{6}$$

k_{a}^{0} can be estimated in analogy to Eq. (4):

$$\frac{k_{\mathrm{a}}^{0}}{k_{\mathrm{a0}}^{0}} = \frac{D}{D_0} \tag{7}$$

where D_0 and D now represent the relative translational diffusion constants of the two proteins without and with crowding. $\Delta\Delta G_{\mathrm{c}}^{\star}$ can be calculated by our postprocessing method.

Applications: interrogation by experiments

The all-atom representation of test proteins, afforded by the postprocessing approach, makes the modeling of crowding

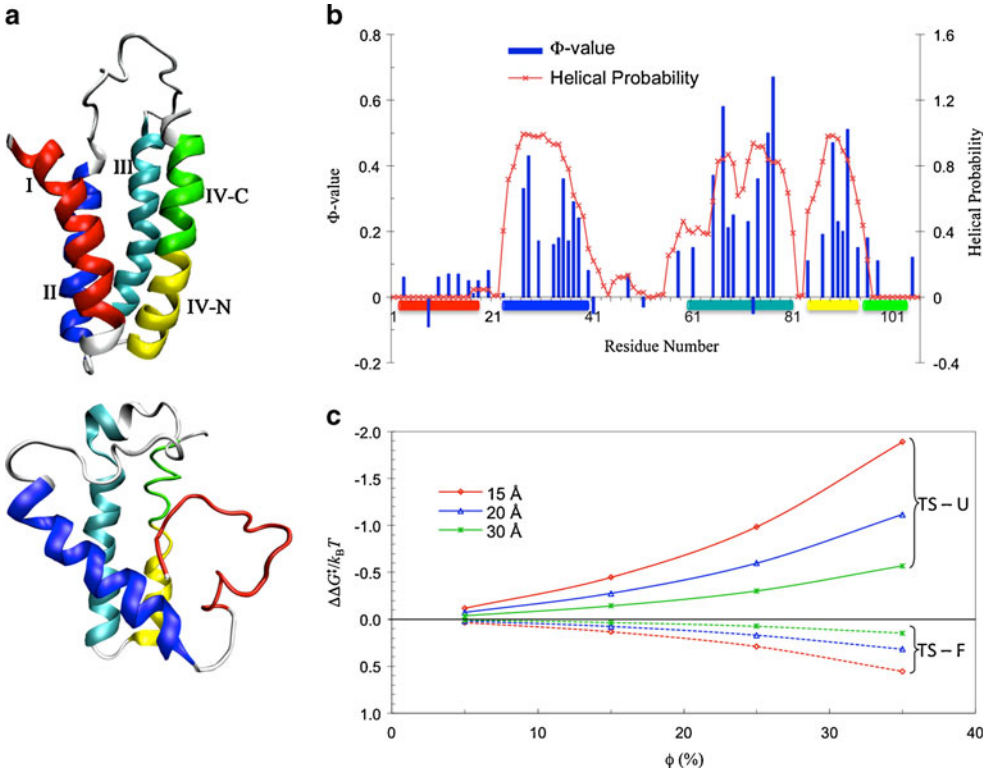

Fig. 4 The folding transition state of cytochrome b_{562} and effects of crowding on its folding and unfolding activation energies, taken from Tjong and Zhou (2010). **a** *Top* The folded state, with helical segments *color coded and labeled*; *bottom* a representative conformation of the transition-state ensemble. **b** Comparison of the residue helical probabilities calculated on the transition-state ensemble with experimental Φ-values (Zhou et al. 2005). **c** Postprocessing results for the effects of crowding on the folding activation energy (*curves* labeled TS – U) and the unfolding activation energy (*curves* labeled TS – F). Results for three crowder radii are shown by the curves in *different colors*

more realistic and reduces the number of adjustable parameters in comparison with experiments. In particular, one no longer has the freedom of adjusting the size of a test protein. Therefore, the interrogation by experiments becomes more quantitative. Below we summarize several applications of the postprocessing approach in modeling the effects of crowding on the thermodynamics and kinetics of protein folding, conformational transition, and binding.

Ai et al. (2006) used the ^{15}N relaxation dispersion technique to determine the folding and unfolding rate constants (k_f and k_u) of cytochrome b_{562} in the absence and presence of 85 g/l PEG 20 K. At 25 °C they observed that crowding caused a 45 % increase in k_f and a very small 6 % decrease in k_u. To quantitatively rationalize these results, we carried out simulations to unfold cytochrome b_{562}, a four-helix bundle protein, by high temperature (Tjong and Zhou 2010). The order of melting of the helices in the simulations was consistent with previous experimental observations (Zhou et al. 2005), leading us to identify the transition-state ensemble as comprising conformations in which helices II, III, and IV-N are partially folded and helices I and IV-C are unfolded (Fig. 4a). The probabilities of individual residues in the helical state (Fig. 4b), calculated on the putative transition-state ensemble, correlated well with experimental Φ-values (Zhou et al. 2005), which measure the extent to which native interactions are formed in the transition state. Applying the postprocessing approach to these conformational ensembles of the folded state, transition state, and unfolded state generated in simulations without crowders, we calculated the effects of crowding on the

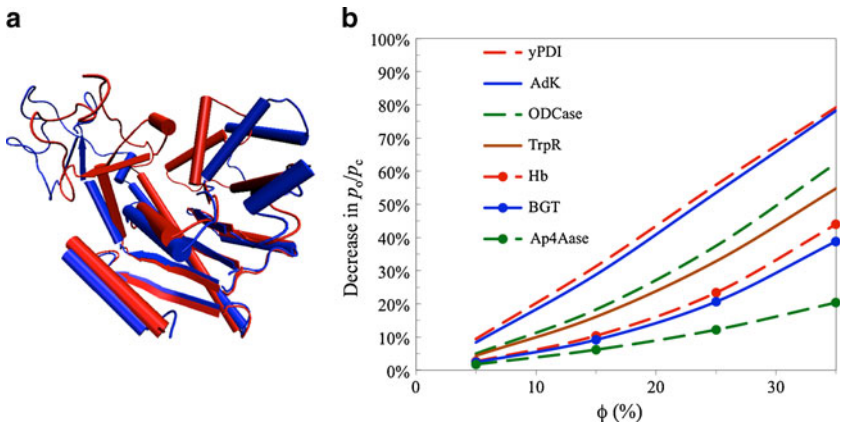

Fig. 5 Effects of crowding on the conformational transition of seven proteins, taken from Dong et al. (2010). **a** Conformational difference between the open (*blue*) and closed (*red*) forms of adenylate kinase (Adk), one of the seven proteins studied. **b** Decreases in the open-to-closed probability ratios of the seven proteins by crowding. The crowder radius was 15 Å

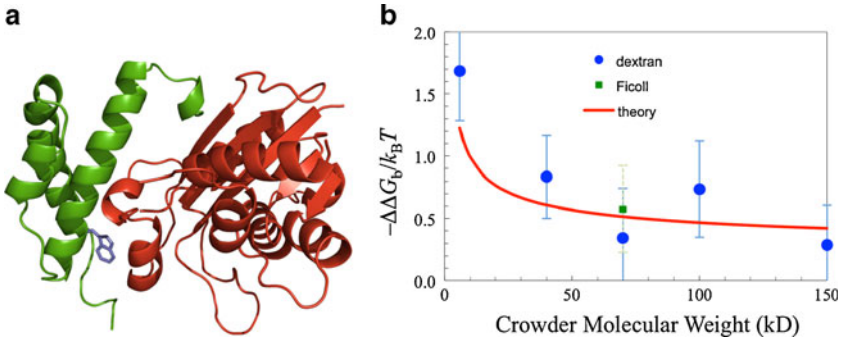

Fig. 6 Effects of crowding on the binding affinity of the DNA polymerase III ε and θ subunits. **a** Structure of the ε-θ complex. ε and θ are given in *red* and *green*, respectively. A tryptophan introduced in the interface as a fluorescence probe is shown. **b** Experimental (*symbols*) and theoretical (*curve*) results for the effects of crowding on the binding free energy

activation energies for folding and unfolding (Fig. 4c). With a crowder size (20 Å) and volume fraction (15 %) approximating the experimental condition (PEG 20 K at 85 g/l), we found a decrease of $0.28k_BT$ in the folding activation energy and an increase of $0.08k_BT$ in the unfolding activation energy. Assuming that the prefactor A is unaffected by crowding, as can be justified according to the preceding section, we would predict a 32 % increase in k_f and a 8 % decrease in k_u, which is in good agreement with the experimental values.

Expanding on our study of crowding effects on the HIV-1 protease dimer flap open equilibrium (Qin et al. 2010), we used the postprocessing approach to study how crowding affects the equilibria and transition rates between open and closed conformations of seven proteins, including adenylate kinase (Fig. 5a) (Dong et al. 2010). For each protein, explicit-solvent molecular dynamics simulations of the open and closed states were separately run, and snapshots were taken to calculate the transfer free energies ($\Delta\mu_o$ and $\Delta\mu_c$). In the presence of 15-Å crowders with a 35 % volume fraction, the open-to-closed probability ratio (p_o/p_c) decreased by 78 % for adenylate kinase. This prediction is consistent with a subsequent experimental study using TMAO as the crowding agent (Nagarajan et al. 2011). Among the seven proteins that we studied, the effects of crowding were reduced when the conformational difference between the open and closed state was less (Fig. 5b). We also calculated the effects of crowding on the potentials of mean force along the open-close reaction coordinate, which suggested that crowding could affect the conformational transition rates.

We carried out experiments to measure the effects of crowding on the binding affinity of the ε and θ subunits of *Escherichia coli* DNA polymerase III (Fig. 6a) (Batra et al. 2009a). Dextran of various molecular weights and Ficoll70 were used as crowding agents, and both were found to increase the binding affinity (Fig. 6b). At the same crowder concentration (100 g/l), the effect of dextran apparently tapered as the molecular weight increased. The experimental results were quantitatively rationalized when 100 g/l dextran with molecular weight W (in kDa) was modeled as crowder with a fixed 15 % volume fraction and radius given by $8.26W^{1/3}$ Å (Fig. 6b).

In a joint experimental-computational study with the Schreiber group, we recently determined the effects of PEG 20 K and dextran 40 K on the association rate constant of two proteins, TEM-1 and BLIP (Fig. 7a) (Phillip et al. 2012a). The association rate constant was essentially

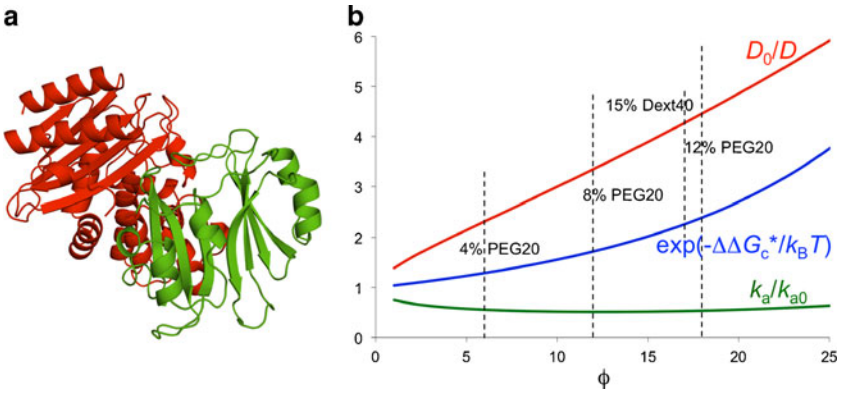

Fig. 7 Effects of crowding on the association rate constant of TEM1 and BLIP, adapted from Phillip et al. (2012a). **a** Structure of the TEM1-BLIP complex. TEM1 and BLIP are given in *red* and *green*, respectively. **b** ϕ dependences of the relative translational diffusion constant (D), the effective interaction energy ($\Delta\Delta G_c^*$), and the association rate constant (k_a), calculated for PEG 20 K. PEG 20 K was modeled as a polymer for D and as a 20-Å crowder for $\Delta\Delta G_c^*$; the correspondence between three PEG weight fractions and volume fractions is indicated by *vertical lines*. Dextran 40 K at 15 % results in a fourfold slowing down in relative diffusion and, when modeled as a 30-Å crowder, leads to a $\Delta\Delta G_c^*$ that translates into a 2.3-fold rate enhancement

unaffected by 4, 8, and 12 % PEG 20 K or 15 % dextran 40 K. We rationalized this observation by our transient-complex theory extended for crowding (Fig. 7b). PEG 20 K at 4–12 % was estimated to slow down the relative diffusion of the two proteins by two- to fivefold. Modeling PEG 20 K as a 20-Å crowder with a volume fraction proportional to the weight fraction, we calculated the crowder-induced interaction energy, $\Delta\Delta G_c^{\star}$, to be $-0.3k_BT$ to $-0.9k_BT$, corresponding to a 1.3- to 2.4-fold rate enhancement. These two opposing factors together lead to the observed null effect of crowding (Fig. 7b). Similar results were obtained for 15 % dextran 40 K (Fig. 7b).

Conclusion

With the ability to represent proteins with atomistic details, we are now much closer in making quantitative predictions on the effects of crowding on the thermodynamics and kinetics of protein folding, conformational transition, and binding. To date, the crowders have only been modeled crudely, mostly as spherical particles with purely repulsive interactions. More sophisticated crowders, with residue-level details and compositions approaching those of bacterial cells, have become computationally feasible (Ando and Skolnick 2010; McGuffee and Elcock 2010; Mereghetti et al. 2010). Combined with the power of the postprocessing approach, we can start to predict, with some confidence, thermodynamic and kinetic properties under in vivo crowding conditions. Integrated with experimental studies (Ghaemmaghami and Oas 2001; Ignatova and Gierasch 2004; Ebbinghaus et al. 2010; Phillip et al. 2012b), we will soon be able to gain new insight into biochemical processes in cellular environments. It will be of particular interest to address questions such as whether protein sequences are tuned for folding or binding in particular cellular compartments.

Acknowledgments This work was supported in part by Grant GM88187 from the National Institutes of Health.

Conflict of interest The authors declare that they have no conflict of interest.

References

Ai X, Zhou Z, Bai Y, Choy WY (2006) ^{15}N NMR spin relaxation dispersion study of the molecular crowding effects on protein folding under native conditions. J Am Chem Soc 128: 3916–3917

Alsallaq R, Zhou HX (2008) Electrostatic rate enhancement and transient complex of protein–protein association. Proteins 71:320–335

Ando T, Skolnick J (2010) Crowding and hydrodynamic interactions likely dominate in vivo macromolecular motion. Proc Natl Acad Sci USA 107:18457–18462

Ansari A, Jones CM, Henry ER, Hofrichter J, Eaton WA (1992) The role of solvent viscosity in the dynamics of protein conformational changes. Science 256:1796–1798

Batra J, Xu K, Qin S, Zhou H-X (2009a) Effect of macromolecular crowding on protein binding stability: modest stabilization and significant biological consequences. Biophys J 97:906–911

Batra J, Xu K, Zhou H-X (2009b) Nonaddtive effects of mixed crowding on protein stability. Proteins 77:133–138

Cheung MS, Klimov D, Thirumalai D (2005) Molecular crowding enhances native state stability and refolding rates of globular proteins. Proc Natl Acad Sci USA 102:4753–4758

Denos S, Dhar A, Gruebele M (2012) Crowding effects on the small, fast-folding protein lambda(6–85). Faraday Discuss 157:451–462

Dhar A, Samiotakis A, Ebbinghaus S, Nienhaus L, Homouz D, Gruebele M, Cheung MS (2010) Structure, function, and folding of phosphoglycerate kinase are strongly perturbed by macromolecular crowding. Proc Natl Acad Sci USA 107:17586–17591

Dong H, Qin S, Zhou HX (2010) Effects of macromolecular crowding on protein conformational changes. PLoS Comput Biol 6: e1000833

Ebbinghaus S, Dhar A, McDonald JD, Gruebele M (2010) Protein folding stability and dynamics imaged in a living cell. Nat Methods 7:319–323

Elcock AH (2010) Models of macromolecular crowding effects and the need for quantitative comparisons with experiment. Curr Opin Struct Biol 20:196–206

Ellis RJ (2001) Macromolecular crowding: obvious but underappreciated. Trends Biochem Sci 26:597–604

Englander SW, Kallenbach NR (1983) Hydrogen exchange and structural dynamics of proteins and nucleic acids. Q Rev Biophys 16:521–655

Feig M, Sugita Y (2012) Variable interactions between protein crowders and biomolecular solutes are important in understanding cellular crowding. J Phys Chem B 116:599–605

Galiano L, Blackburn ME, Veloro AM, Bonora M, Fanucci GE (2009) Solute effects on spin labels at an aqueous-exposed site in the flap region of HIV-1 protease. J Phys Chem B 113:1673–1680

Ghaemmaghami S, Oas TG (2001) Quantitative protein stability measurement in vivo. Nat Struct Biol 8:879–882

Ignatova Z, Gierasch LM (2004) Monitoring protein stability and aggregation in vivo by real-time fluorescent labeling. Proc Natl Acad Sci USA 101:523–528

Kim YC, Best RB, Mittal J (2010) Macromolecular crowding effects on protein-protein binding affinity and specificity. J Chem Phys 133:205101

Kornberg A (2000) Ten commandments: lessons from the enzymology of DNA replication. J Bacteriol 182:3613–3618

Kuttner YY, Kozer N, Segal E, Schreiber G, Haran G (2005) Separating the contribution of translational and rotational diffusion to protein association. J Am Chem Soc 127:15138–15144

Lebowitz JL, Rowlinson JS (1964) Thermodynamic properties of mixtures of hard spheres. J Chem Phys 41:133–138

McGuffee SR, Elcock AH (2010) Diffusion, crowding & protein stability in a dynamic molecular model of the bacterial cytoplasm. PLoS Comput Biol 6:e1000694

Mereghetti P, Gabdoulline RR, Wade RC (2010) Brownian dynamics simulation of protein solutions: structural and dynamical properties. Biophys J 99:3782–3791

Miklos AC, Sarkar M, Wang Y, Pielak GJ (2011) Protein crowding tunes protein stability. J Am Chem Soc 133:7116–7120

Minh DD, Chang CE, Trylska J, Tozzini V, McCammon JA (2006) The influence of macromolecular crowding on HIV-1 protease internal dynamics. J Am Chem Soc 128:6006–6007

Minton AP (1981) Excluded volume as a determinant of macromolecular structure and reactivity. Biopolymers 20:2093–2120
Minton AP (1998) Molecular crowding: analysis of effects of high concentrations of inert cosolutes on biochemical equilibria and rates in terms of volume exclusion. Methods Enzymol 295:127–149
Minton AP (2000) Effect of a concentrated "inert" macromolecular cosolute on the stability of a globular protein with respect to denaturation by heat and by chaotropes: a statistical-thermodynamic model. Biophys J 78:101–109
Minton AP (2005) Models for excluded volume interaction between an unfolded protein and rigid macromolecular cosolutes: macromolecular crowding and protein stability revisited. Biophys J 88:971–985
Mittal J, Best RB (2010) Dependence of protein folding stability and dynamics on the density and composition of macromolecular crowders. Biophys J 98:315–320
Nagarajan S, Amir D, Grupi A, Goldenberg DP, Minton AP, Haas E (2011) Modulation of functionally significant conformational equilibria in adenylate kinase by high concentrations of trimethylamine oxide attributed to volume exclusion. Biophys J 100:2991–2999
Oversteegen SM, Roth R (2005) General methods for free-volume theory. J Chem Phys 122:214502
Phillip Y, Sherman E, Haran G, Schreiber G (2009) Common crowding agents have only a small effect on protein-protein interactions. Biophys J 97:875–885
Phillip Y, Harel M, Khait R, Qin S, Zhou HX, Schreiber G (2012a) Contrasting factors on the kinetic path to protein complex formation diminish the effects of crowding agents. Biophys J 103:1011–1019
Phillip Y, Kiss V, Schreiber G (2012b) Protein-binding dynamics imaged in a living cell. Proc Natl Acad Sci USA 109:1461–1466
Qin S, Zhou H-X (2009) Atomistic modeling of macromolecular crowding predicts modest increases in protein folding and binding stability. Biophys J 97:12–19
Qin S, Zhou HX (2010) Generalized fundamental measure theory for atomistic modeling of macromolecular crowding. Phys Rev E 81:031919
Qin S, Minh DD, McCammon JA, Zhou HX (2010) Method to predict crowding effects by postprocessing molecular dynamics trajectories: application to the flap dynamics of HIV-1 protease. J Phys Chem Lett 1:107–110
Qin S, Mittal J, Zhou HX (2013) Folding free energy surfaces of three small proteins under crowding: validation of the postprocessing method by direct simulation. Phys Biol (in press)
Qin S, Pang X, Zhou HX (2011) Automated prediction of protein association rate constants. Structure 19:1744–1751
Qin S, Cai L, Zhou HX (2012) A method for computing association rate constants of atomistically represented proteins under macromolecular crowding. Phys Biol 9:066008
Qu Y, Bolen DW (2002) Efficacy of macromolecular crowding in forcing proteins to fold. Biophys Chem 101–102:155–165
Roberts A, Jackson SE (2007) Destabilised mutants of ubiquitin gain equal stability in crowded solutions. Biophys Chem 128:140–149
Rosenfeld Y (1989) Free-energy model for the inhomogeneous hard-sphere fluid mixture and density-functional theory of freezing. Phys Rev Lett 63:980–983
Schlarb-Ridley BG, Mi H, Teale WD, Meyer VS, Howe CJ, Bendall DS (2005) Implications of the effects of viscosity, macromolecular crowding, and temperature for the transient interaction between cytochrome f and plastocyanin from the cyanobacterium Phormidium laminosum. Biochemistry 44:6232–6238
Spencer DS, Xu K, Logan TM, Zhou H-X (2005) Effects of pH, salt, and macromolecular crowding on the stability of FK506-binding protein: an integrated experimental and theoretical study. J Mol Biol 351:219–232
Tjong H, Zhou HX (2010) The folding transition-state ensemble of a four-helix bundle protein: helix propensity as a determinant and macromolecular crowding as a probe. Biophys J 98:2273–2280
Ueda Y, Taketomi H, Go N (1978) Studies on protein folding, unfolding, and fluctuations by computer simulation. II. A. Three-dimensional lattice model of lysozyme. Biopolymers 17:1531–1548
Widom B (1963) Some topics in theory of fluids. J Chem Phys 39:2808–2812
Yuan J-M, Chyan C-L, Zhou H-X, Chung T-Y, Peng H, Ping G, Yang G (2008) The effects of macromolecular crowding on the mechanical stability of protein molecules. Protein Sci 17:2156–2166
Zhou H-X (2004) Protein folding and binding in confined spaces and in crowded solutions. J Mol Recognit 17:368–375
Zhou HX (2010) Rate theories for biologists. Q Rev Biophys 43:219–293
Zhou HX (2013) Polymer crowders and protein crowders act similarly on protein folding stability. FEBS Lett http://dx.doi.org/10.1016/j.febslet.2013.01.030
Zhou Z, Huang Y, Bai Y (2005) An on-pathway hidden intermediate and the early rate-limiting transition state of Rd-apocytochrome b562 characterized by protein engineering. J Mol Biol 352:757–764
Zhou HX, Rivas G, Minton AP (2008) Macromolecular crowding and confinement: biochemical, biophysical, and potential physiological consequences. Annu Rev Biophys 37:375–397
Zimmerman SB, Minton AP (1993) Macromolecular crowding: biochemical, biophysical, and physiological consequences. Annu Rev Biophys Biomol Struct 22:27–65